Deep Coupled GAN-Based Score-Level Fusion for Multi-Finger Contact to Contactless Fingerprint Matching

Md Mahedi Hasan
Lane Department of Computer Science and Electrical Engineering
West Virginia University
Morgantown, WV, USA
mh00062@mix.wvu.edu

Nasser Nasrabadi
Lane Department of Computer Science and Electrical Engineering
West Virginia University
Morgantown, WV, USA
nasser.nasrabadi@mail.wvu.edu

Jeremy Dawson
Lane Department of Computer Science and Electrical Engineering
West Virginia University
Morgantown, WV, USA
jeremy.dawson@mail.wvu.edu

2022 International Conference of the Biometrics Special Interest Group (BIOSIG) | 978-1-6654-7666-9/22/$31.00 ©2022 IEEE | DOI: 10.1109/BIOSIG55365.2022.9897056

***Abstract*—Interoperability between contact to contactless images in fingerprint matching is a key factor in the success of contactless fingerprinting devices, which have recently witnessed an increasing demand for biometric authentication. However, due to the presence of perspective distortion and the absence of elastic deformation in contactless fingerphotos, direct matching between contactless fingerprint probe images and legacy contact-based gallery images produces a low accuracy. In this paper, to improve interoperability, we propose a coupled deep learning framework that consists of two Conditional Generative Adversarial Networks. Generative modeling is employed to find a projection that maximizes the pairwise correlation between these two domains in a common latent embedding subspace. Extensive experiments on three challenging datasets demonstrate significant performance improvements over the state-of-the-art methods and two top-performing commercial off-the-shelf SDKs, i.e., Verifinger 12.0 and Innovatrics. We also achieve a high-performance gain by combining multiple fingers of the same subject using a score fusion model.**

***Index Terms*—contactless fingerphoto recognition, fingerprint interoperability, coupled GAN**

I. Introduction

A contact-based fingerprint biometric system can be vulnerable to latent fingerprints from the impression of previous subjects, low-contrast regions due to the presence of dust and dirt on the sensor platen, and the high risk of infection with the SARS-CoV-2 virus. Furthermore, contact-based fingerprints also suffer from elastic deformation due to the uneven distribution of pressure onto the platen which severely affects the ridge patterns [1]. To address these limitations, a contactless fingerphoto device has been proposed [2] which does not require any specialized sensor technologies and produces images free of elastic deformation [3]. The success of contactless fingerphoto devices depends on their ability to match against legacy contact-based fingerprint databases.

However, most of the previous cross-domain matching algorithms are designed to improve the interoperability between contact to contactless fingerprints using only images from a single finger [4], [5]. In fact, very few comprehensive studies are found in the literature on multi-finger contactless fingerphoto matching. In this paper, we devise several strategies to effectively utilize the multi-finger input from a subject for improving interoperability.

In recent years, deep learning algorithms have been extensively used in cross-sensor fingerprint matching [5]–[8]. Many of these methods employed a Siamese-like network to directly compare the contact-based fingerprint to a contactless fingerphoto [5]–[7]. However, it is inherently difficult to learn a consistent deep representation from the contactless fingerphotos because of the perspective distortion occurring in the peripheral areas of the fingerphotos. In addition, direct matching using a Siamese-like network is also not efficient, as the Siamese network is not rich enough to learn a similarity metric in a cross-domain matching scenario.

In this study, we hypothesize that a contactless fingerphoto and a contact-based fingerprint possess a latent similarity in a low-dimensional feature subspace. So, to exploit this latent similarity, we project both the fingerphoto and the fingerprint into a common embedding subspace using a coupled learning framework that uses Generative Adversarial Networks (GANs) [9]. The goal of the research presented in this paper is to build a framework based on a Coupled GAN (CpGAN) architecture [10] to find the hidden relationship between the feature embedding of each domain for cross-domain fingerprint matching. Likewise, the framework can also apply to improve interoperability in intra-domain cross-sensor matching. The main contributions of this paper are:

- A coupled GAN cross-domain (contact to contactless) fingerprint recognition model for more accurate cross-matching.
- A multi-finger contact-based fingerprint versus multi-finger contactless fingerphoto matching framework for increased interoperability during cross-matching.
- Extensive experiments on three challenging datasets, and a comparison of the proposed CpGAN model with the state-of-the-art methods and two top-performing commercial off-the-shelf (COTS) matchers.

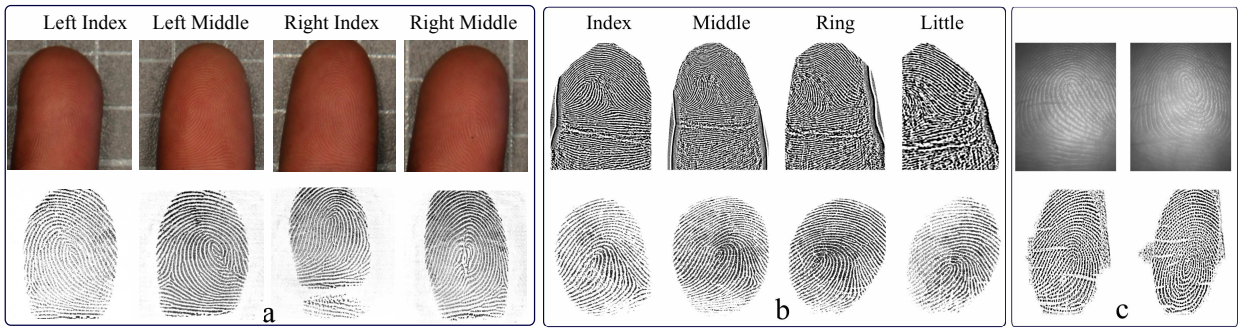

Fig. 1. Some example images of contactless and contact-based fingerprint pairs. (a) A Multimodal Dataset, (b) Non-Contact Fingerprint Dataset-v1, (c) PolyU Contactless Database.

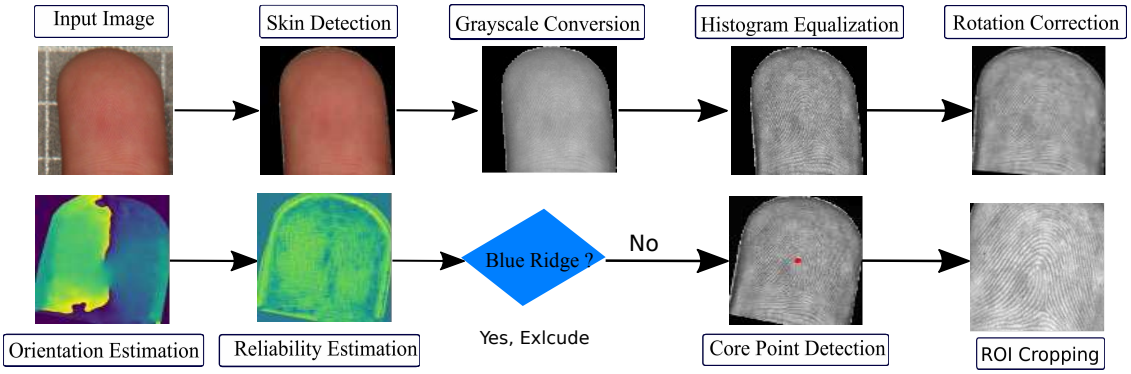

Fig. 2. Overview of the preprocessing steps: segmenting the skin from background, histogram equalization, rotation correction, reliability estimation, and ROI cropping. The steps will effectively remove the differences between the contact-based fingerprints and the contactless fingerphotos such as color, size, and orientation.

II. Related Work

Several early works have been performed in the past decade to develop novel algorithms to improve the interoperability between contact-based fingerprint and contactless fingerphoto sensors [4]–[6], [8]. Lin et al. [4] presented a deformation correction model to correct the deformation on the fingerphotos for contact to contactless matching. Recently, they proposed a multi-Siamese network [5] with a distance-aware loss function to accurately match a fingerphoto with a contact-based fingerprint. Their framework consists of three sub-networks. Each of the sub-networks has two inputs: fingerphoto and fingerprint. The fingerprint representation vectors from these sub-nets are concatenated for a more accurate cross-domain matching. A minutiae attention network based on a Siamese architecture and a reciprocal distance loss function was proposed in [6]. Although these networks achieved a remarkable improvement over the state-of-the-art approaches, their application is limited due to the challenges associated with cross-domain matching. Specifically, the large intra-class variation due to the significant differences in sensing technologies makes it more difficult for Siamese-like networks to tackle, as the Siamese architecture is mainly designed for learning a similarity metric in the same domain.

In recent years, GAN architectures [9] have been widely adopted for applications like cross-domain image generation [11] and synthetic fingerprint generation [12], [13], etc. These techniques provide an effective way to map a source distribution into a target distribution by learning a generator network, G, and a discriminator network, D, using a min-max optimization game. The conditional GAN (cGAN) was introduced by Mirza et al. [14] where both the generator and the discriminator are conditioned on an additional input, such as labels, texts, or images. Liu [10] proposed a Coupled GAN, a framework that consists of a pair of GANs, each of which is responsible for generating images in one domain.

In our work, we employ a Coupled GAN framework which consists of two cGANs and a multi-loss objective function. In contrast to extracting handcrafted minutiae-based features for direct comparison, in this method, we project both the contactless fingerphoto and contact-based fingerprint in to a common low-dimensional embedding subspace using the generative modeling [9] of the coupled GAN framework for indirect matching.

III. Proposed Method

In this section, we elaborate on our proposed method for cross-domain fingerprint recognition. As shown in Figure 3, the proposed method is constructed using a coupled framework

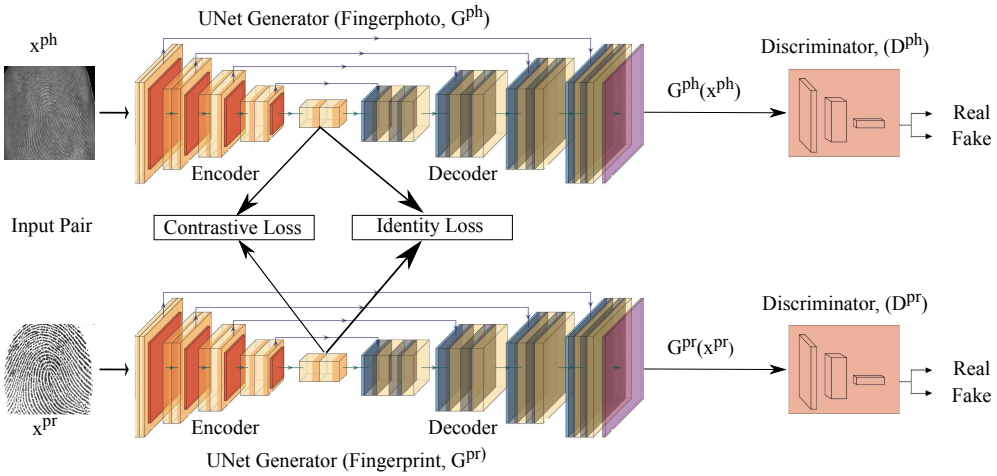

Fig. 3. Block diagram of the proposed Coupled GAN architecture. It consists of two conditional GAN sub-networks. The generators of both GANs use the same architecture that allows matching both domains in an embedded low-dimensional feature space.

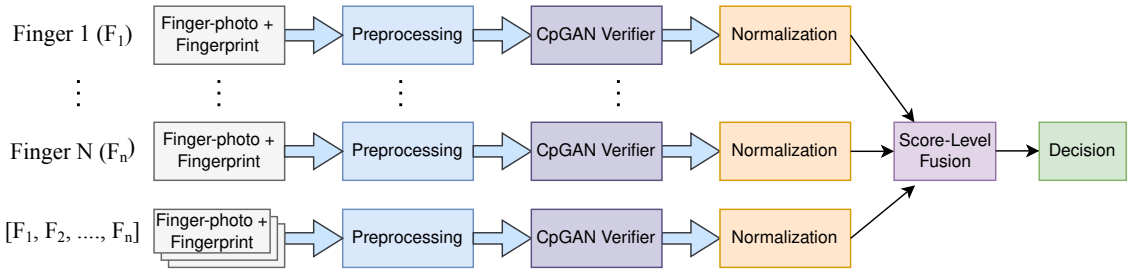

Fig. 4. The block diagram of the proposed score fusion model for multi-finger cross-domain matching. For each finger, we train a dedicated CpGAN verifier, and we train another CpGAN verifier by concatenating the fingerphotos and the fingerprints of all the fingers in a channel-wise manner.

that consists of two sub-networks, where each sub-network is a cGAN architecture made up of a generator and a discriminator.

A. Preprocessing

We have performed an elaborate preprocessing scheme to reduce the variations of fingerprints from different sensors. Figure 2 illustrates the overview of the key preprocessing steps. First, we segmented the skin from the background of an input image, then converted the image to grayscale to perform histogram equalization. Afterward, an accurate rotation correction was performed. To make sure that both the fingerprints and fingerphotos are similar, these steps were applied to both the fingerphotos and fingerprints.

Due to the image capturing process of contactless fingerphotos, some of the ridges of the minutiae points are quite blurry which leads us to perform a quality assessment to discard the bad quality images. Hence, our second preprocessing step is only applied to the fingerphotos, which is made up of orientation and reliability estimation. In reliability estimation, if the edges of these fingerphoto images are not well defined, they were excluded from the dataset. Otherwise, the algorithm moves on to core point detection and ROI cropping. The output size for all images was scaled to 256x256 pixels. In addition to preprocessing, we performed normalization to make samples align to the standard resolution, i.e., 500 DPI. We also performed heavy data augmentation like random rotation, horizontal flipping, and random cropping to increase the amount of the training data.

B. Network Architecture

Our proposed CpGAN framework, as illustrated in Figure 3, consists of two cGAN sub-networks. The fingerphoto sub-network is dedicated to reconstructing the synthetic fingerphoto image. Similarly, the fingerprint sub-network is only dedicated to the fingerprint reconstruction. Each cGAN sub-network is composed of a generator and a discriminator, and each generator is composed of an encoder and a decoder. These two sub-networks are connected by a contrastive loss that compares the embedded feature vectors of the two encoders. To optimize the network effectively, we create one imposter pair for every genuine pair. The total loss function for this model is given by Eqn 3. The dimension of the embedded feature vector is $1,024$.

For multi-finger matching, we propose a score fusion model, as illustrated in Figure 4. For each finger position, we train a dedicated CpGAN model using the fingerphoto and fingerprint pair of that finger. Then, we train another CpGAN model by concatenating the fingerphotos and the fingerprints of all the

TABLE I
STATISTICS OF MULTIMODAL DATASET. IT SHOWS THE NUMBER OF SUBJECTS AND IMAGE PAIRS AFTER PREPROCESSING STEPS ARE APPLIED.

Set	Dataset	Subject	Finger	Impression
Train	Multimodal-2012	714	2106	2106
Test	Multimodal-2013	286	1218	1218

TABLE II
STATISTICS OF THE NON-CONTACT FINGERPRINT DATASET-V1. WE RESERVED THIS DATASET ONLY TO EVALUATE THE CPGAN ON COMMERCIAL FINGERPHOTO VS CROSSMATCH GUARDIAN MATCHING.

Set	Subject	Finger	Impression
Test	129	516	516

fingers in a channel-wise manner. The output of the model is then normalized using min-max normalization and then averaged to produce a single score, as shown in Figure 4.

C. CpGAN Objective Function

In this study, we employ the contrastive loss function (L_{cont}). It pulls the genuine pairs (i.e., inputs from the same subject) toward each other in a common embedding subspace, and, concurrently, pushes the impostor pairs (i.e., inputs from different subjects) away from each other. Let x^{ph} (x^{pr}) is the input fingerphoto (fingerprint), z^{ph} (z^{pr}) is the latent embedding of fingerphoto (fingerprint), and Y denote the label of the input pairs. If the input pairs (x^{ph}, x^{pr}) belong to the same subject (a genuine pair), then $Y = 0$, and $Y = 1$ if they belong to the two different subjects (an imposter pair). The term $D_w(x^{ph}, x^{pr})$ represents the L_2-norm distance to measure the similarities between the output vectors (z^{ph}, z^{pr}) generated by mapping (x^{ph}, x^{pr}) to their corresponding latent, respectively. If m denotes the margin that defines a radius on the embedding space, then the contrastive loss can be defined by the following equation:

$$L_{const} = (Y)\frac{1}{2}\{max(0, (m - D_w(x^{ph}, x^{pr})\}^2 + (1 - Y)\frac{1}{2}D_w(x^{ph}, x^{pr})^2. \quad (1)$$

Furthermore, we have utilized the adversarial loss [9] to train the generators and the discriminators of both conditional GANs. Let D^{ph} be the discriminator of the fingerphoto cGAN and D^{pr} be the discriminator of the fingerprint cGAN. Now, using the notions of Eqn 1, the adversarial loss for both of the cGANs is given as:

$$\begin{aligned} L_{adv}^{ph} &= \min_G \max_D [\mathbb{E}_{y^{ph}\sim P_d(y)}[\log D^{ph}(y^{ph}|x^{ph})] + \\ &\quad \mathbb{E}_{z\sim P_z(z)}[\log(1 - D^{ph}(G^{ph}(z|x^{ph})))]], \\ L_{adv}^{pr} &= \min_G \max_D [\mathbb{E}_{y^{pr}\sim P_d(y)}[\log D^{pr}(y^{pr}|x^{pr})] + \\ &\quad \mathbb{E}_{z\sim P_z(z)}[\log(1 - D^{pr}(G^{pr}(z|x^{pr})))]]. \end{aligned} \quad (2)$$

Total adversarial loss is the combination of these two losses. Here, y^{ph} (y^{pr}) denotes the real fingerphoto (fingerprint) data.

TABLE III
COMPILED DATASET FOR PRETRAINING THE CPGAN MODEL FOR CONTACTLESS FINGERPHOTO VS CONTACT-BASED FINGERPRINT MATCHING.

Dataset	Subject	Finger	Impression
Multimodal-2009	1,098	10,907	31,297
Multimodal-2012	791	7,903	22,088
NIST 302	200	2,000	7,701
Total	2,089	20,810	**61,086**

TABLE IV
COMPILED DATASET FOR PRETRAINING THE CPGAN MODEL FOR COMMERCIAL FINGERPHOTO VS CROSSMATCH GUARDIAN MATCHING.

Dataset	Subject	Finger	Impression
Multimodal-2009	1,098	10,907	31,297
Multimodal-2012	791	7,903	22,088
Multimodal-2013	286	2,860	16,549
Total	2,175	21,670	**69,934**

It is worth mentioning that y^{ph} (y^{pr}) and the condition given by x^{ph} (x^{pr}) are the same.

In addition to the adversarial loss, we also employ identity loss calculated from the latent embedding subspace of the fingerphoto and the fingerprint cGAN modules. It helps to build a more discriminative embedding subspace that further enhances the performance of cross-domain fingerprint recognition. To calculate the loss, we first subtract the latent embedding vectors and then feed them into a softmax layer of two neurons. Finally, the binary cross-entropy loss is calculated from the outputs of the softmax layer.

The L_2 loss measures the reconstruction error between the synthesized fingerprint and the corresponding input fingerprint image. The overall objective function of our proposed CpGAN model is given as the summation of all the above-mentioned losses.

$$L_{total} = L_{cons} + \lambda_1 L_{ident} + \lambda_2 L_{adv} + \lambda_3 L_2, \quad (3)$$

where λ_1, λ_2, and λ_3 are the hyperparameters to control the effect of each loss function.

IV. EXPERIMENTS AND RESULTS

In this section, we briefly describe the training datasets and the protocol setup for our experiments. Then, we show the efficacy of our proposed CpGAN method for cross-domain fingerprint matching by comparing its performance with the commercial off-the-shelf matchers and the state-of-the-art methods such as Minutiae Attention [6]. We also explore the effect of combining multi-fingers on interoperability using our score fusion model.

A. Datasets

We train the CpGAN model on an in-house fingerprint dataset called the Multimodal Dataset (2008, 2009, 2012, 2013). It consists of four subsets. The Multimodal-2012 is a set of 791 subjects and a total of $69,934$ impression pairs, whereas, the Multimodal-2013 contains 286 subjects and a total of $16,549$ impression pairs. Each subject, in both of

TABLE V

COMPARISON BETWEEN CPGAN AND TWO TOP-RANKING COMMERCIAL OFF-THE-SHELF MATCHERS FOR INDIVIDUAL FINGERPHOTO VS ITS CORRESPONDING FINGERPRINT MATCHING ON THE MULTIMODAL-2013 DATASET. OUR PROPOSED CPGAN MODEL WITH U-NET BASED GENERATOR PERFORMS SLIGHTLY BETTER THAN THE COMMERCIAL MATCHERS ON BOTH TEST IMAGES AND INDIVIDUAL FINGER POSITIONS. ADDITIONALLY, AMONG DIFFERENT FINGER POSITIONS, THE INDEX FINGER OF BOTH HANDS PERFORMS SLIGHTLY BETTER THAN OTHER FINGERS.

Set	Finger Position	Train Images	Test Images	Network	Proposed CpGAN		Verifinger 12.0		Innovatrics	
					AUC(%)	EER(%)	AUC(%)	EER(%)	AUC(%)	EER(%)
Test	All	2106	1218	ResNet-18	99.55	2.38	96.73	4.83	98.64	4.33
				U-Net	**99.59**	**2.38**				
				DenseNet	99.45	2.38				
Individual	**2**	423	228	U-Net	**99.60**	2.23	97.86	**1.93**	99.25	2.30
	3	362	215		98.92	4.19	96.91	3.82	**98.93**	**2.38**
	4	310	192		**98.92**	**5.21**	97.35	5.40	96.53	9.96
	7	404	230		**99.55**	**2.17**	97.40	3.20	99.41	2.76
	8	350	193		**99.17**	4.66	96.99	**4.51**	98.89	4.88
	9	257	160		**98.41**	**5.63**	93.90	8.33	96.67	8.46

TABLE VI

COMPARISON BETWEEN THE SCORE FUSION MODEL AND THE COMMERCIAL OFF-THE-SHELF MATCHER ON MULTI-FINGERPHOTOS VS MULTI-FINGERPRINTS MATCHING.

# of Fingers	Finger Position	Train Images	Test Images	Score Fusion		Innovatrics	
				AUC(%)	EER(%)	AUC(%)	EER(%)
2	2,3	263	174	**99.70**	**1.72**	98.96	3.03
2	3,4	209	146	**99.52**	**2.74**	97.64	8.86
2	7,8	239	160	99.76	1.87	**99.99**	**0.00**
2	8,9	183	111	99.68	2.70	**99.99**	**0.00**
3	2,3,7	185	145	**99.88**	**1.38**	97.55	2.92
3	2,3,4	166	119	**99.90**	**1.68**	97.29	2.92
3	3,7,8	158	117	99.99	0.00	99.99	0.00
4	**2,3,7,8**	139	98	100.0	0.00	100.0	0.00

these datasets, has a varying number of fingers from a total of six available fingers: right index (2), right middle (3), right ring (4), left index (7), left middle (8), and left ring (9). The contact-based set consists of 800x750-sized fingerprints with a resolution of 500 PPI and the contactless set consists of fingerphotos of size 512x512 with similar resolution to fingerprints. In contrast, the Multimodal-2009 contains only a total of 31,297 fingerprint images and the Multimodal-2008 contains only finger roll images.

In our first experiment, we tested our CpGAN model for contact to contactless matching on the Multimodal dataset. Table I shows the statistics of the Multimodal Dataset. Due to rigorous image quality assessment, a significant number of bad-quality images were excluded. To pretrain the proposed model, we also built a compiled dataset, shown in Table III. In addition, for multi-finger matching, we combine two, three, and four individual fingers of a subject (see Table VI).

To further evaluate the cross-matching performance of our proposed framework on a commercial fingerphoto device and the Crossmatch Guardian fingerprint, we employed another in-house dataset called the Non-Contact Fingerprint Dataset-v1. Table II shows the statistics of the dataset. A total of 516 impression pairs are available from the left index (7), left middle (8), left ring (9), and left little (10) finger.

To comparatively evaluate the performance of our proposed framework, we also tested our model on the PolyU dataset [4]. It has a total of 2,880 contact to contactless impressions pairs from 320 individual fingers. We employed the standard experimental settings [4], [6], [8], i.e., 160 fingers each with 12 impression pairs are set for training, and the remaining 160 fingers, each with 6 impression pairs, are set for testing. Figure 1 depicts a set of samples of these three aforementioned datasets.

B. Implementation Details

We implement the U-Net architecture [15] as the generator for both the fingerphoto and the fingerprint cGAN modules. In the experiment on a held-out validation set, we empirically set the hyper-parameter $\lambda_1 = 10$, $\lambda_2 = 1$ and $\lambda_3 = 1$. We employ the Adam optimizer [16] with an initial learning rate of 0.0002. We use the ReLU activation for the generator and the Leaky ReLU [17] with a slope of 0.20 for the discriminator. Due to the lack of a large training dataset, it is very hard to train the whole network directly for convergence. So, we pretrain both of the fingerprint cGAN modules of our Coupled GAN framework using a compiled dataset (see Table III) like a Siamese framework by sharing their weights. We then employ this pretrained cGAN module to initialize both the fingerprint and the fingerphoto cGAN modules of the proposed CpGAN framework.

C. Performance Evaluation on Individual Fingerprint Matching

As shown in Table V, our proposed CpGAN model obtains an area under curve (AUC) score of 99.59% on the Multimodal-2013 Dataset which is 2.95% higher than Verifinger 12.0 and 0.96% higher than Innovatrics. It also achieves an equal error rate (EER) score which is 50.72% and 45.03% lower than Verifinger 12.0 and Innovatrics matchers, respectively. In our work, we have experimented with several generator architectures such as ResNet-18 [18], U-Net [15], and DenseNet [19]. However, the performance of these different generators is almost similar. Furthermore, Table V verifies that the proposed CpGAN performs better than the commercial matchers on individual finger positions. For example, on the left ring finger, we achieve an AUC score that is 4.80% higher than Verifinger 12.0 and 1.79% higher than Innovatrics.

TABLE VII

COMPARISON WITH THE COMMERCIAL OFF-THE-SHELF MATCHERS FOR INDIVIDUAL FINGERPHOTO VS GUARDIAN FINGERPRINT MATCHING ON THE NON-CONTACT FINGERPRINT DATASET-V1. OUR PROPOSED CPGAN MODEL OUTPERFORMS THE COMMERCIAL MATCHERS ON BOTH THE TEST SET AND THE INDIVIDUAL FINGER POSITIONS.

Set	Finger Position	Test Images	Network	Proposed CpGAN		Verifinger 12.0		Innovatrics	
				AUC(%)	EER(%)	AUC(%)	EER(%)	AUC(%)	EER(%)
Test	All	516	ResNet-18	97.33	6.59	94.65	11.12	97.07	6.90
			UNET	97.37	6.59				
			DenseNet	97.13	6.59				
Individual	7	129	U-Net	**98.76**	3.88	97.46	4.96	98.73	**3.45**
	8	129		**97.41**	**4.65**	94.52	8.76	96.88	6.83
	9	129		**98.18**	**5.43**	96.21	6.93	98.11	5.98
	10	129		92.05	15.50	88.01	21.01	**93.15**	**13.12**

TABLE VIII

COMPARISON WITH COMMERCIAL OFF-THE-SHELF MATCHERS ON THE NON-CONTACT FINGERPRINT DATASET-V1 FOR MULTI-FINGER COMMERCIAL FINGERPHOTOS VS MULTI-FINGER GUARDIAN FINGERPRINTS MATCHING PROVES THAT THE PROPOSED SCORE FUSION MODEL PERFORMS BETTER THAN THE COMMERCIAL MATCHERS IN ALL MULTI-FINGER COMBINATION. THE BEST PERFORMANCE IS ACHIEVED FROM FOUR FINGER MATCHING.

Number of Fingers	Finger Position	Test Images	Proposed Score Fusion		Innovatrics	
			AUC(%)	EER(%)	AUC(%)	EER(%)
2	7,8	129	**99.02**	2.86	98.77	2.86
2	8,9	129	**98.61**	3.39	98.47	3.39
2	9,10	129	**97.98**	5.12	97.94	5.12
3	7,8,9	129	**99.14**	2.63	98.95	2.63
3	8,9,10	129	**98.73**	3.31	98.66	3.31
4	**7,8,9,10**	129	**99.24**	2.17	99.18	2.17

TABLE IX

COMPARISON BETWEEN THE CPGAN AND THE STATE-OF-THE-ART METHODS ON THE POLYU DATASET. OUR PROPOSED CPGAN MODEL OUTPERFORMS OTHERS AT A SIGNIFICANT MARGIN. IT ACHIEVES 8.9% LOWER EER SCORE THAN THE PREVIOUS BEST MINUTIAE ATTENTION MODEL.

Methods	EER (%)
Verifinger 12.0	19.31
Multi-Siamese CNN [5]	7.11
Minutiae Attention [6]	4.13
Proposed CpGAN	**3.76**

In addition, as shown in Table VI, the performance of multi-finger fusion of our proposed score fusion model is slightly better than the commercial matchers. As the number of fingers from the same subject used for multi-finger fusion increases, the performance of our score fusion model and the commercial matchers also increases. In particular, we obtain perfect verification performance (AUC=1.0 and EER=0.0) when we combine four fingers.

We employed the Non-Contact Fingerprint Dataset-v1 to evaluate our CpGAN model on commercial fingerphotos after pretraining it on another compiled dataset (see Table IV). The verification performance on this dataset is illustrated in Table VII. It has been observed that the CpGAN model outperforms the commercial matchers by a noticeable margin based on both AUC and EER scores. In multi-finger fusion, as observed in Table VIII, our proposed score fusion model achieves significantly higher scores than the commercial matchers. Furthermore, as shown in Table IX, the experiment of our proposed method using the PolyU [4] dataset also shows a significant improvement over the state-of-the-art methods such as Multi-Siamese CNN [5] and Minutiae Attention [6]. Our method achieves 8.9% lower EER score than the previous best Minutiae Attention method [6] on the PolyU dataset.

TABLE X

COMPARISON AMONG DIFFERENT NUMBER OF FINGERS CONFIRMS THAT MULTI-FINGER MATCHING USING PROPOSED SCORE FUSION MODEL SIGNIFICANTLY IMPROVES THE INTEROPERABILITY.

Experiment		1v1	2v2	3v3	4v4
Fingerphoto vs Fingerprint	Position	2	2,3	2,3,7	2,3,7,8
	AUC(%)	99.60	99.65	97.71	**100.0**
	EER(%)	2.23	1.72	1.38	**0.00**
Commercial photo vs Guardian	Position	7	7,8	7,8,9	7,8,9,10
	AUC(%)	98.76	99.02	99.14	**99.24**
	EER(%)	03.88	02.86	02.63	**02.17**

D. Performance Evaluation on Multi-Finger Fingerprint Matching

The impact of multi-finger on contact to contactless fingerprint matching of our proposed score fusion framework is demonstrated in Table X. Figure 5-6 illustrates the effects of multi-finger matching based on the receiver operating characteristic (ROC) and detection error trade-off (DET) curves for different combination of multi-finger matching. From the ROC and DET curves in Figure 5-6, we see that as the number of fingers increases the performance of contact to contactless fingerprint matching also gradually increases, and the four finger fusion gives us the best AUC and EER scores. Therefore, the experimental results prove that combining multiple fingers of the same subject significantly improves the interoperability of cross-domain fingerprint matching.

V. CONCLUSION

We proposed a new framework, CpGAN, for matching contact to contactless fingerprints from different sensors for improving the interoperability. We thoroughly evaluated the proposed CpGAN model on several challenging datasets. From our performance evaluation, we observe that our proposed CpGAN model, after pretraining on a large, compiled fingerprint dataset, achieves significantly better results than the state-of-the-art methods presented in the literature and the commercial

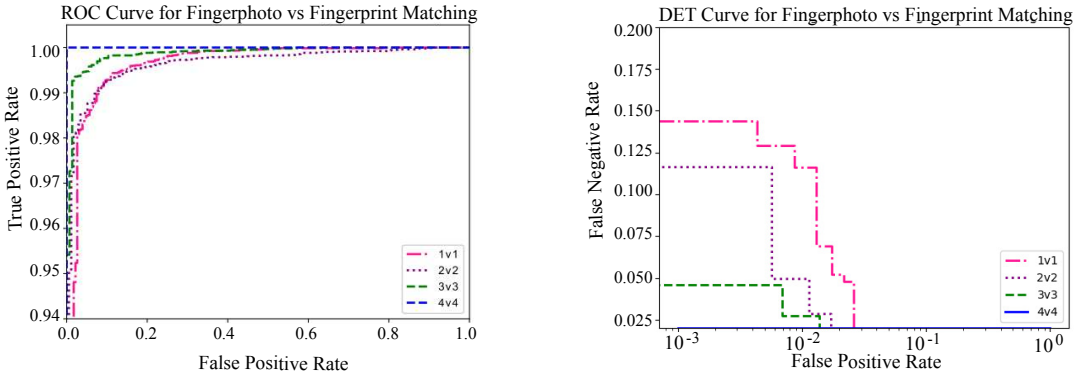

Fig. 5. ROC and DET curve of our proposed method for contact and contactless fingerprint matching on the Multimodal 2013 Dataset.

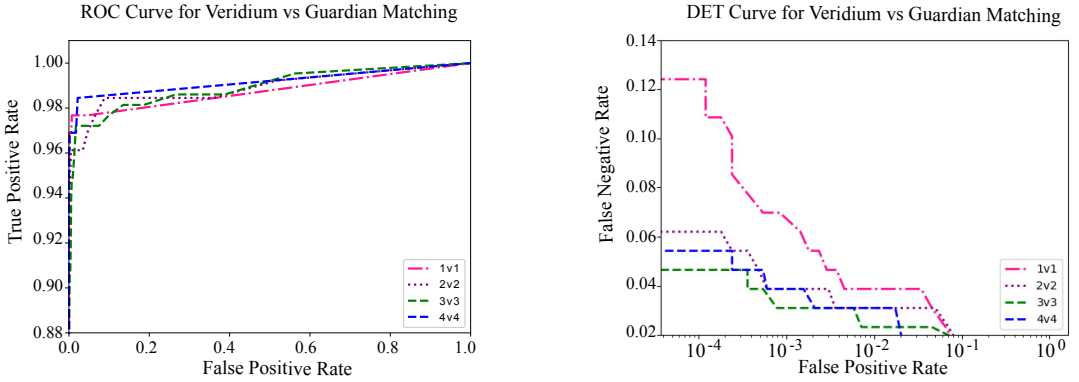

Fig. 6. ROC and DET curve of our proposed method for commercial fingerphotos vs Guardian fingerprint matching on the Non-Contact Fingerprint Dataset-v1.

off-the-shelf matchers. It also demonstrates the effectiveness of implementing comprehensive data preprocessing and multiple loss functions. Furthermore, the experiments using our proposed score fusion model on multi-finger settings show further improvement in interoperability.

ACKNOWLEDGMENT

This material is based upon a work supported by the Center for Identification Technology Research and the National Science Foundation under Grant 1650474.

REFERENCES

[1] J. Priesnitz, C. Rathgeb, N. Buchmann, C. Busch, and M. Margraf, "An overview of touchless 2d fingerprint recognition," *EURASIP Journal on Image and Video Processing*, vol. 2021, no. 1, pp. 1–28, 2021.

[2] Y. Song, C. Lee, and J. Kim, "A new scheme for touchless fingerprint recognition system," in *Int. Sym. on Intel. Signal Proces. and Com. Sys.*, 2004, pp. 524–527.

[3] J. Libert, J. Grantham, B. Bandini, S. Wood, M. Garris, K. Ko, and et al., "Guidance for evaluating contactless fingerprint acquisition devices," *NIST Spec. Publ*, 2018.

[4] C. Lin and A. Kumar, "Matching contactless and contact-based conventional fingerprint images for biometrics identification," *IEEE Trans. on Image Proc.*, vol. 27, no. 4, pp. 2008–2021, 2018.

[5] C. Lin and A. Kumar, "A cnn-based framework for comparison of contactless to contact-based fingerprints," *IEEE Trans. Inf. Forensics Security*, vol. 14, no. 3, pp. 662–676, 2019.

[6] H. Tan and A. Kumar, "Minutiae attention network with reciprocal distance loss for contactless to contact-based fingerprint identification," *IEEE Trans. Inf. Forensics Security*, vol. 16, pp. 3299–3311, 2021.

[7] A. Alrashidi, A. Alotaibi, M. Hussain, H. AlShehri, H. AboAlSamh, and G. Bebis, "Cross-sensor fingerprint matching using siamese network and adversarial learning," *Sensors*, vol. 21, no. 11, p. 3657, 2021.

[8] S. Grosz, J. Engelsma, E. Liu, and A. Jain, "C2cl: contact to contactless fingerprint matching," *IEEE Trans. Inf. Forensics Security*, 2021.

[9] I. Goodfellow, J. Pouget-Abadie, M. Mirza, B. Xu, D. Warde-Farley, S. Ozair, and et al., "Generative adversarial nets," in *Neural Information Processing Systems (NIPS)*, 2014.

[10] M. Liu and O. Tuzel, "Coupled generative adversarial networks," *Advances in neural information processing systems*, vol. 29, 2016.

[11] Y. Taigman, A. Polyak, and L. Wolf, "Unsupervised cross-domain image generation," in *5th International Conference on Learning Representations*, 2017.

[12] S. Minaee and A. Abdolrashidi, "Finger-gan: generating realistic fingerprint images using connectivity imposed gan," *arXiv preprint arXiv:1812.10482*, 2018.

[13] J. Engelsma, S. Grosz, and A. Jain, "Printsgan: synthetic fingerprint generator," *arXiv preprint arXiv:2201.03674*, 2022.

[14] M. Mirza and S. Osindero, "Conditional generative adversarial nets," *arXiv preprint arXiv:1411.1784*, 2014.

[15] O. Ronneberger, P. Fischer, and T. Brox, "U-net: convolutional networks for biomedical image segmentation," in *MICCAI*, 2015, pp. 234–241.

[16] D. Kingma and J. Ba, "Adam: a method for stochastic optimization," in *3rd Int. Conf. on Learning Representations*. San, Diego, 2015.

[17] B. Xu, N. Wang, T. Chen, and M. Li, "Empirical evaluation of rectified activations in convolutional network," *arXiv preprint arXiv:1505.00853*, 2015.

[18] K. He, X. Zhang, S. Ren, and J. Sun, "Deep residual learning for image recognition," in *CVPR*, 2016, pp. 770–778.

[19] G. Huang, Z. Liu, L. Maaten, and K. Weinberger, "Densely connected convolutional networks," in *CVPR*, 2017, pp. 4700–4708.